Taniguchi et al., https://doi.org/10.1083/jcb.201704085

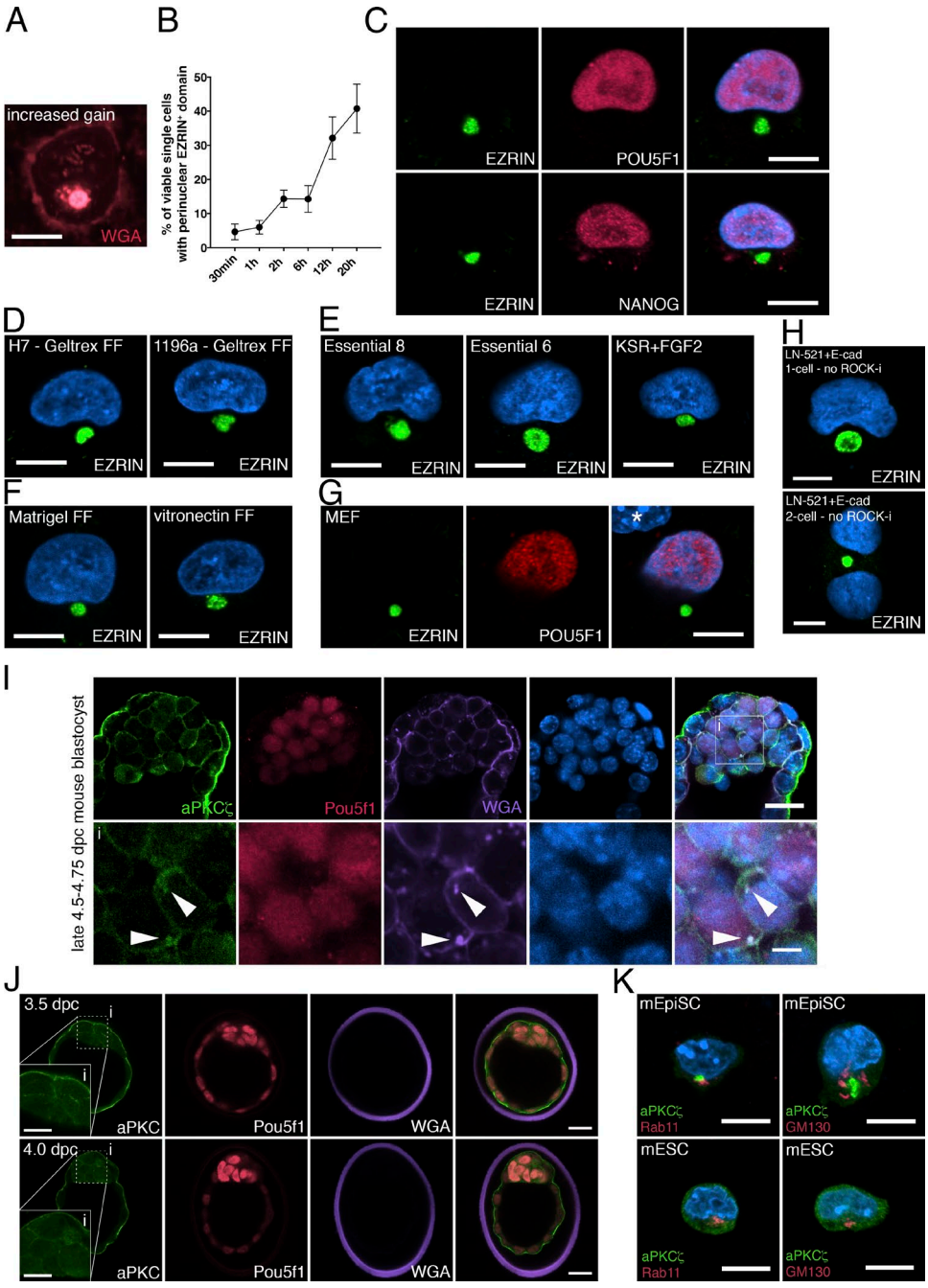

Figure S1. **Formation of the apicosome in a variety of conditions.** (A) Red channel (WGA staining) of the image in Fig. 1 A with increased gain to reveal outer plasma membrane staining. (B) Percentage of viable single H9 cells containing a perinuclear EZRIN+ domain at various time points between 30 min and 20 h after plating. 50 cells were counted from three independent samples (total 150) per time point. Error bars indicate SD. This experiment was repeated two times. (C) Confocal images of isolated H9 cells stained for EZRIN (green) and POU5F1 or NANOG (red). (D) Apicosomes in H7 (WA07, a distinct hESC line) and the 1196a human iPSC line, grown for 20 h on a Geltrex feeder-free layer and immunostained for EZRIN (green). (E) EZRIN-stained (green) H9 cells grown for 20 h in Essential 8 (left), Essential 6 (middle), and a common hPSC medium (DMEM/F12 with 10% KSR and FGF2, right). (F and G) EZRIN-stained (green) H9 cells grown for 20 h on different substrates: Matrigel (F, left), vitronectin (F, right), or an MEF feeder layer (G). In G, the asterisk indicates an MEF that lacks POU5F1 expression. (H) EZRIN-stained (green) H9 cells grown for 20 h on a laminin-521/E-cadherin matrix substrate. Apicosome formation is seen in 37.3 ± 3.1% (n = 3, triplicate of 50 cells) of isolated cells (as judged by perinuclear EZRIN localization). (I) Fluorescent confocal images of late 4.5- to 4.75-dpc mouse blastocysts, stained with indicated markers. Arrowheads indicate intracellular accumulations of aPKCζ and membrane (WGA). (J) Confocal images of 3.5- and 4.0-dpc blastocysts stained with indicated markers. The ICM domain is magnified further (inset) in the green channel (aPKCζ). (K) Apicosomes in single mEpiSC and mESC stained with indicated markers. Bars: (A–H, J, and K) 10 µm; (I) 20 µm; (I-i and J-i) 5 µm. For all images, blue indicates DNA staining (HOECHST).

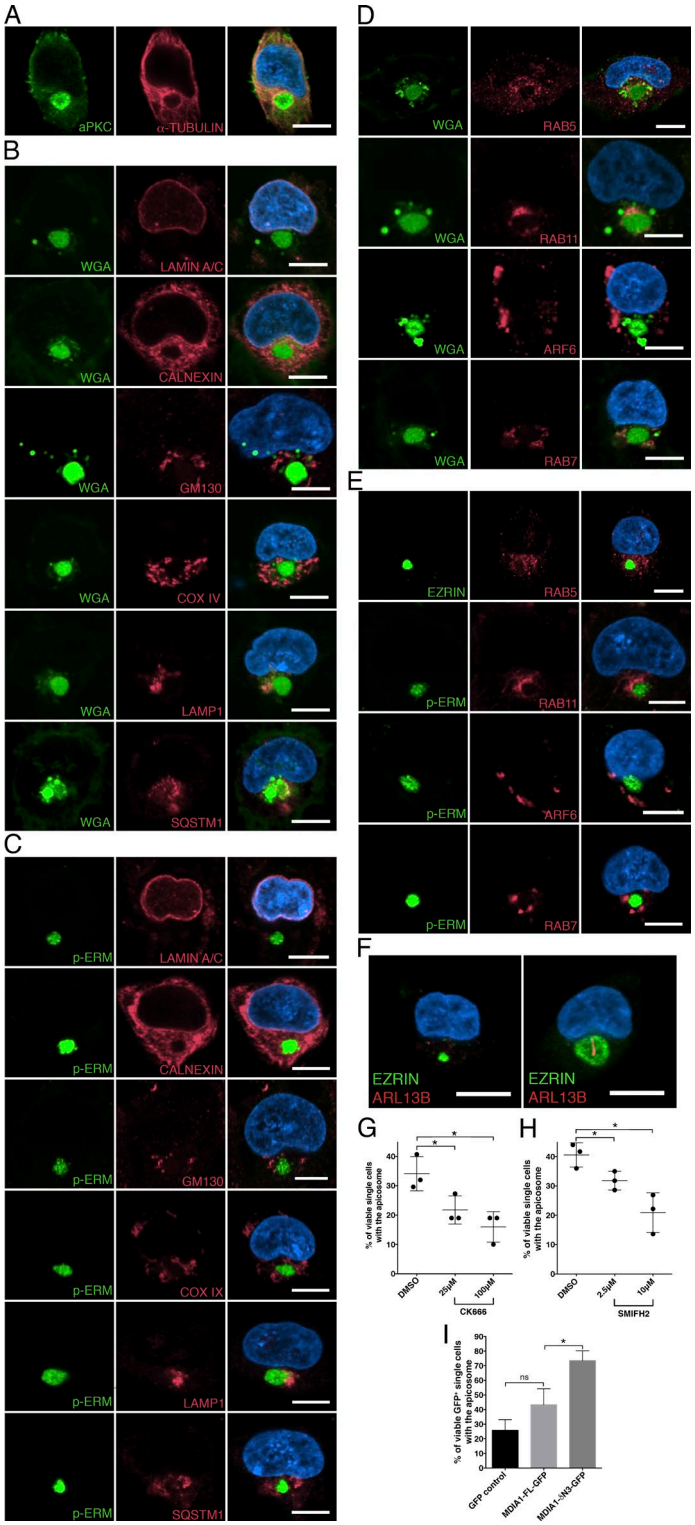

Figure S2. **Characterization of the apicosome.** (A) Singly isolated H9 cell stained for aPKCζ and α-TUBULIN (microtubule marker). (B–E) Singly isolated H9 cells stained for WGA (membrane marker, green, B and D) or apical marker p-ERM (green, C and E) in addition to antibodies specific to distinct organelles (red, individual channels of Fig. 1, F and G): LAMIN A/C (nucleus), CALNEXIN (ER), GM130 (Golgi), COX IV (mitochondria), LAMP1 (lysosome), SQSTM1 (autophagosome), RAB5 (early endosome), RAB11 (recycling endosome), ARF6 (recycling endosome), and RAB7 (late endosome). (F) Confocal images of dissociated H9 clones stained for EZRIN (green) and ARL13B (red), showing cells with small (left) and large (right) apicosomes. The cell in the right panel is identical to the cell in Fig. 2 C. (G and H) H9 clones treated with graded concentrations of CK666 (ARP2/3 inhibitor, G) or SMIFH2 (formin inhibitor, H) for 20 h in standard culture conditions containing ROCK-i. Presence of the apicosome (as judged by perinuclear EZRIN localization) is quantified. 50 cells were counted from three independent samples (total 150) per condition. This experiment was repeated two times. (I) H9 clones expressing GFP, mDIA1-FL-GFP, or mDIA-δN3-GFP and costained for EZRIN were quantitated for the presence of the apicosome (perinuclear EZRIN$^+$ complex) 20 h after plating. 50 cells were counted from three independent samples (total 150) per cell line. This experiment was repeated two times. Bars, 10 µm. For all images, blue indicates DNA staining (HOECHST). For G–I, error bars indicate SD. Student's *t* test was used for statistical analysis: NS > 0.05; *, $P \leq 0.05$.

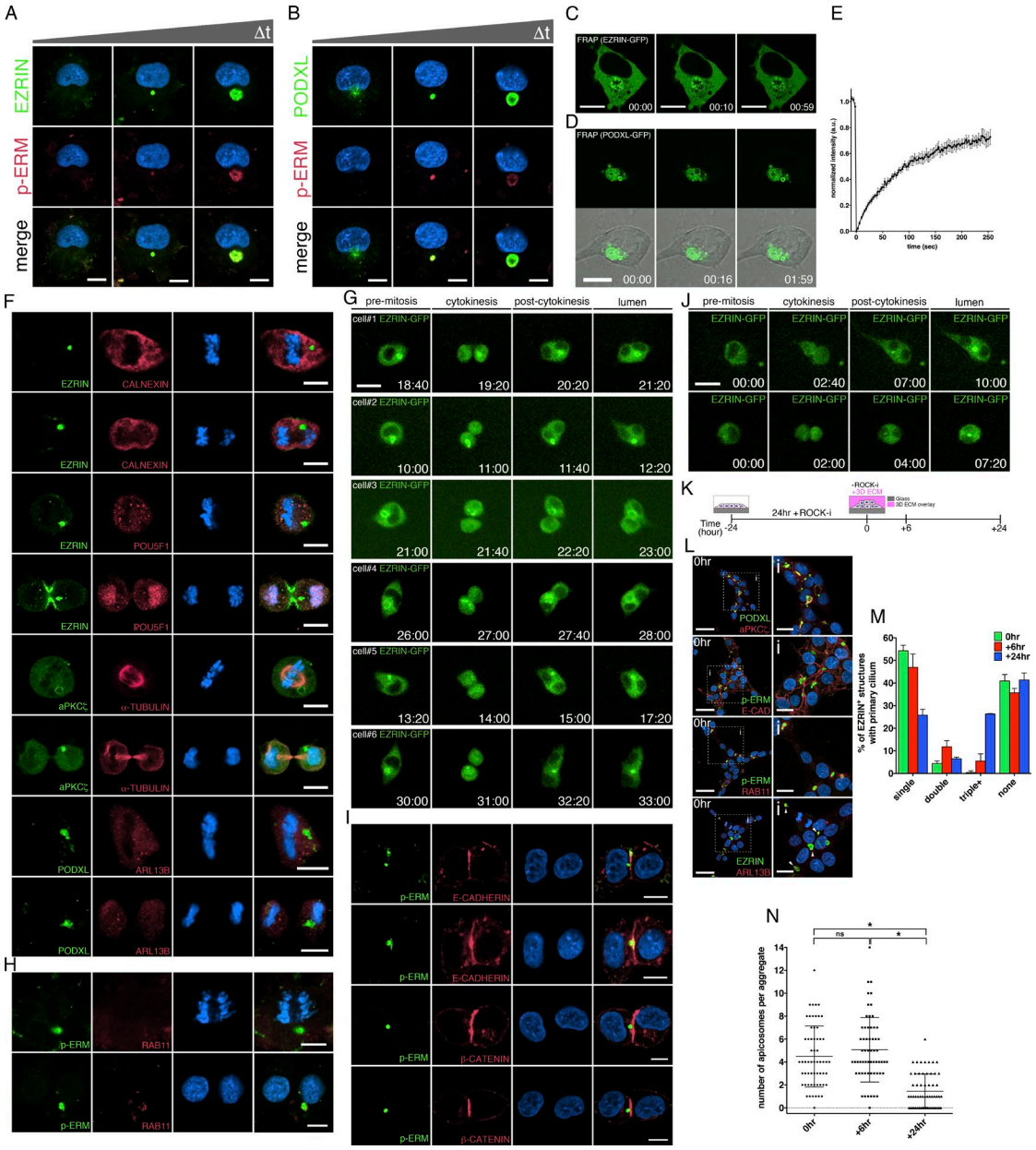

Figure S3. **Characterization of apicosome dynamics.** (A and B) De novo formation of the apicosome over time. Isolated H9 cells were harvested at different time points (30 min, 2 h, 6 h, and 24 h after plating) and costained with antibodies specific to EZRIN (green, A) or PODXL (green, B) in addition to p-ERM (red). The perinuclear domain marked by diffuse PODXL at 30 min (B, left-most panels), does not costain with p-ERM antibodies. (C and D) FRAP analysis using EZRIN–GFP (top; Video 5) and PODXL–GFP (bottom; Video 6) cells. Dotted circle indicates where photobleaching was applied. Time stamp, min:s. (E) Quantitation of the FRAP analysis of PODXL–GFP cells. Values are plotted using normalized fluorescent recovery values obtained from 10 quantitated cells. Error bars indicate SEM. (F) Presence of the apicosome during mitosis. Mitotic H9 single cells are stained using indicated markers (individual channels of Fig. 4 C). (G) Asymmetric segregation of the apicosome during mitosis. Live imaging of six independent single H9 cells stably expressing an EZRIN–GFP transgene. Time stamp, h:min. (H) RAB11 localization in mitotic and postmitotic cells. Isolated H9 cells are stained using indicated markers. (I) The apicosome inserts into the cytokinetic plane. Mitotic H9 single cells are stained for p-ERM (green) with E-CADHERIN (red) or β-CATENIN (red), individual channels in Fig. 4 (E and F). (J) Delayed apicosome formation, initiated after cell division in isolated cells that did not form an apicosome before mitosis (see premitosis). Representative live imaging of two independent single H9 EZRIN–GFP cells (Video 9). An apicosome appears in one daughter (see postcytokinesis) after cytokinesis is complete. (K) Schematic of the hPSC-aggregate lumen formation assay in Fig. 5 A. Singly dissociated H9 cells were plated at six times higher density than single isolated cells in the presence of ROCK-i (Y-27632, at −24). After 24 h (0 h, higher magnification images in L), ROCK-i was removed from the medium, and cells were replenished with medium containing 2% Geltrex (+3D ECM). Analysis was performed on cells that were harvested before ROCK-i withdrawal (Fig. 5, B–E, top row, 0 h) or on cells that were harvested 6 h (Fig. 5, B–E, middle row) or 24 h (Fig. 5, B–E, bottom row) after ROCK-i withdrawal. (L) Characterization of the hPSC aggregates at 0 h (higher magnification images of 0 h in Fig. 5, B–E). Dotted boxes (i) indicate magnified regions. Arrowheads indicate apicosomes studded with one primary cilium (ARL13B staining). (M) Ciliary dynamics in hPSC aggregates. Quantitation of the fraction of EZRIN$^+$ structures containing single, double, more than three (triple$^+$), or no (none) primary cilium in hPSC aggregates at 0 h (green), +6 h (red), and +24 h (blue) after ROCK-i withdrawal. 20 aggregates were analyzed per independent sample (total 60 aggregates). Error bars indicate SD. This experiment was repeated two times. (N) Quantitation of the number of apicosomes per aggregate at 0, +6, and +24 h ROCK-i withdrawal time points. The data used to plot this graph are from M. Error bars indicate SD. Student's *t* test was used for statistical analysis: NS > 0.05; *, $P \leq 0.05$. Bars: (A–D, F, H, and I) 10 µm; (G and J) 25 µm; (L) 50 µm; (L-i) 20 µm. Blue indicates DNA staining (HOECHST).

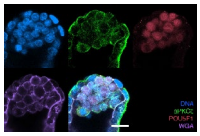

Video 1. **Serial confocal scans (11 total scans, 1 µm per scan) of late E4.5- to E4.75-dpc mouse blastocysts from Fig. S1 I, stained with indicated markers.** White arrowheads indicate intracellular accumulations of aPKCζ and membrane (WGA).

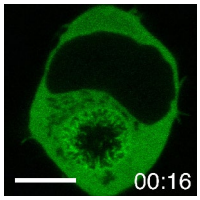

Video 2. **Time-lapse imaging of a singly plated EZRIN–GFP cell containing an apicosome.** This movie shows the highly dynamic nature of the apicosome and shows that EZRIN is localized inside of the apicosome because of abundant lumenally projected microvilli. Time stamp, min:s.

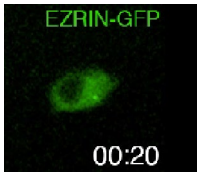

Video 3. **Time-lapse imaging of the cell shown in Fig. 3, A (EZRIN–GFP) and B (PODXL–GFP).** Time stamp, h:min.

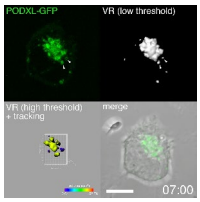

Video 4. **Time-lapse imaging of the PODXL–GFP cell shown in Fig. 3 C (imaging started 30 min after plating).** 3D reconstruction of images (5 × 1-µm interval optical sections per frame) is shown for the GFP channel (top left) and VR at low threshold (top right) or high threshold (bottom left). Merged images (GFP/phase) are shown at bottom right. Low-threshold VR analysis (top right) permits visualization of smaller GFP^{low} vesicles that are being actively trafficked and undergoing fusion events. High-threshold VR analysis (bottom left) allows individual tracking of large GFP^{high} vesicles within the dense perinuclear GFP population (Imaris 7.6; Bitplane). Time stamp, min:s.

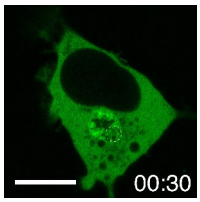

Video 5. **Time-lapse imaging of the EZRIN–GFP cell shown in Fig. S3 C during FRAP.** Time stamp, min:s.

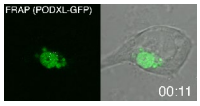

Video 6. **Time-lapse imaging of the PODXL–GFP cell shown in Fig. S3 D during FRAP.** Time stamp, min:s.

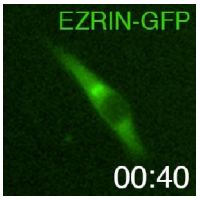

Video 7. **Time-lapse imaging of the cell shown in Fig. 4 A.** Time stamp, h:min.

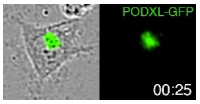

Video 8. **Time-lapse imaging of the cells shown in Fig. 4 B.** Time stamp, h:min.

Video 9. **Time-lapse imaging of the cell shown in Fig. S3 J, top (cell 1) and bottom (cell 2).** Time stamp, h:min.

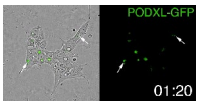

Video 10. **Time-lapse imaging of a cell aggregate shown in Fig. 5 F.** Time stamp, h:min.

Provided online is Table S1, showing a quantitation of the fate of each EZRIN- and PODXL-GFP cell during time-lapse imaging in Fig. 3 (A and B) and Fig. 4 (A and B).